THE JOURNAL OF BIOLOGICAL CHEMISTRY VOL. 287, NO. 39, pp. 32312–32323, September 21, 2012

Rabex-5 Protein Regulates the Endocytic Trafficking Pathway of Ubiquitinated Neural Cell Adhesion Molecule L1*

Received for publication, April 20, 2012, and in revised form, July 20, 2012 Published, JBC Papers in Press, July 30, 2012, DOI 10.1074/jbc.M112.374322

Yoshikatsu Aikawa[1]

From the Laboratory of Neural Membrane Biology, Graduate School of Brain Science, Doshisha University, 1-3 Miyakodani, Kyotanabe, Kyoto 610-0394, Japan

Background: The endocytic trafficking pathway for L1 proteolytic degradation following L1-L1 homophilic binding remains unclear.
Results: Changes in Rabex-5 expression alter the dynamics of ubiquitinated L1 endocytic trafficking.
Conclusion: Rabex-5 has an essential role in the endocytic trafficking of ubiquitinated L1.
Significance: The motif interacting with ubiquitin (MIU) domain, not the A20 ZnF domain, in Rabex-5 controls the endocytic trafficking of ubiquitinated cargo.

Ubiquitination of integral membrane proteins is a common posttranslational modification used to mediate endocytosis and endocytic sorting of cell surface proteins in eukaryotic cells. Ubiquitin (Ub)-binding proteins (UBPs) regulate the stability, function, and localization of ubiquitinated cell surface proteins in the endocytic pathway. Here, I report that the immunoglobulin superfamily cell adhesion molecule L1 undergoes ubiquitination and dephosphorylation on the plasma membrane upon L1 antibody-induced clustering, which mimics L1-L1 homophilic binding, and that these modifications are critical for obtaining the maximal rate of internalization and trafficking to the lysosome, but not to the proteasome. Notably, L1 antibody-induced clustering leads to the association of ubiquitinated L1 with Rabex-5, a UBP and guanine nucleotide exchange factor for Rab5, via interaction with the motif interacting with Ub (MIU) domain, but not the A20-type zinc finger domain. This interaction specifically depends on the presence of an Ub moiety on lysine residues in L1. Rabex-5 expression accelerates the internalization rates of $L1^{WT}$ and $L1^{Y1176A}$, a tyrosine-based motif mutant, but not $L1^{K11R}$, an ubiquitination-deficient mutant, leading to the accumulation of ubiquitinated L1 on endosomes. In contrast, RNA interference-mediated knockdown of Rabex-5 impairs the internalizations of $L1^{WT}$ and $L1^{Y1176A}$, but not $L1^{K11R}$ from the plasma membrane. Overall, these results provide a novel mechanistic insight into how Rabex-5 regulates internalization and postendocytic trafficking of ubiquitinated L1 destined for lysosomal degradation.

L1 is an immunoglobulin superfamily cell adhesion molecule implicated in a number of developmentally important processes, including neuronal cell migration, axon outgrowth, and axon fasciculation (1, 2). It is well established that endocytic retrieval from the rear of the growth cone maintains an L1 gradient across the growth cone and provides a pool of vesicular L1 available for local exocytosis (3–5). The endosomal trafficking is also required to target L1 properly to the growing axon. L1/neuron-glia cell adhesion molecule reaches the axon indirectly by transcytosis, involving initial somatodendritic targeting followed by endocytosis and trafficking to the axon from somatodendritic endosomes (6–8). L1 endocytosis is substrate-dependent process and occurs as a consequence of L1-L1 homophilic binding. The cytoplasmic tail of L1 contains a tyrosine-based recognition motif (YRSLE) that mediates binding to the AP-2 clathrin endocytosis adaptor (5). L1-L1 homophilic binding causes dephosphorylation of this tyrosine-based motif and triggers endocytosis via recruitment of AP-2 (9). In contrast, binding to AP-2 is reduced upon phosphorylation of the tyrosine-based motif downstream of Src signaling (9). Although the dynamic nature of L1-L1 homophilic binding has been studied in detail by using sophisticated live imaging and quantitative tracking approaches (10), the molecular components of postendocytic delivery to lysosomes for down-regulation upon L1-L1 homophilic binding are yet to be identified and characterized.

Posttranslational attachment of ubiquitin (Ub)[2] to polypeptides has a fundamental role in modulating the plasma membrane protein composition (11–13). The current paradigm (supported by studies on chimeric receptor-Ub fusion proteins in yeast and mammalian cells) suggests that ubiquitination promotes the internalization and sorting of cargo receptors by recruiting Ub-binding proteins (UBPs), which link cargo to components of endocytic and sorting machinery (14–16). A number of UBPs, including Rabex-5, present at endosomes are able to participate in degradative sorting of ubiquitinated cargo (14–16). Rabex-5, originally identified as a rabaptin-5-interacting protein, possesses GEF activity for Rab5 (17). It is a multidomain protein consisting of an A20-type zinc finger (ZnF) fused to a motif interacting with Ub (MIU) domain at the N

* This work was supported by Grant-in-aid for Young Scientists (B) (20790085) from the Japan Society for the Promotion of Science, the Uehara Memorial Foundation, and individual research allowances from Doshisha University (to Y. A.). Measurement and data analyses were done at Kagawa School, Tokushima Bunri University.
[1] To whom correspondence should be addressed. Tel.: 81-774-65-6877; E-mail: yaikawa@mail.doshisha.ac.jp.

[2] The abbreviations used are: Ub, ubiquitin; CHX, cycloheximide; EGFP, enhanced GFP; GEF, guanine nucleotide exchange factor; MIU, motif interacting with Ub; UBP, Ub-binding protein; ZnF, zinc finger.

terminus, membrane-binding motif, and tandem helical bundle-VPS9 domains at the center, and a coiled coil region at the C terminus. Rabex-5 binds Ub through the tandem ZnF and MIU UBDs and undergoes UBD-coupled monoubiquitination driven by ZnF Ub-ligase activity (18, 19). Rabex-5 GEF activity is mediated by the helical bundle-VPS9 tandem domains (20). The coiled coil region of Rabex-5 forms a complex with rabaptin-5 and indirectly targets Rabex-5 to early endosomes via rabaptin-5 binding to Rab5-GTP (21, 22). The multidomain architecture of Rabex-5 allows it to perform dual roles in cargo sorting by simultaneously binding to the Ub-binding and ubiquitinated adaptors and promoting Rab5-dependent endosomal fusion.

In this study, I investigated Rabex-5 function in the regulation of internalization, sorting, and lysosomal degradation of ubiquitinated L1 upon L1-L1 homophilic binding. I report that incubation with an L1 antibody (L1-Ab) that mimics L1-L1 homophilic binding leads to ubiquitination and dephosphorylation at the tyrosine-based motif, which facilitates endocytosis via recruitment of Rabex-5. Interfering with L1 ubiquitination reduces L1 internalization due to impairment of the interaction with Rabex-5. It is, therefore, plausible that Rabex-5 plays an important role in neuronal function by controlling L1 internalization and endocytic sorting.

EXPERIMENTAL PROCEDURES

Reagents and Plasmids—Antibodies were purchased against FLAG (M2; Sigma-Aldrich), Myc (9E10 hybridoma; Roche Applied Science), hemagglutinin (HA; Covance Research Products), Ub (Dako Cytomation Denmark A/S, Glostrup, Denmark), FK1 (BioMol, recognizes poly-Ub chains only (23)), GAPDH (Santa Cruz Biotechnology), and L1 (goat polyclonal IgG; Santa Cruz Biotechnology). Affinity-purified polyclonal anti-Rabex-5, anti-Rab5, and anti-L1 antibodies were raised using a C-terminal fragment of bovine Rabex-5 (residues 426–481), full-length human Rab5a, and full-length rat L1 as immunogens, respectively. Mouse monoclonal anti-L1 antibody (74-5H7), rat monoclonal anti-mouse L1 antibody, and rabbit polyclonal anti-human L1 antibody were provided by Dr. V. Lemmon (University of Miami School of Medicine, Miami, FL). Secondary antibodies conjugated to HRP were purchased from Pierce. Alexa Fluor 488-, Alexa Fluor 563-, and Alexa Fluor 633-conjugated secondary antibodies and LysoTracker Red DND-99 were obtained from Molecular Probes. Bafilomycin A1, MG-132, and lactacystin synthetic were obtained from Calbiochem. Protein G-Sepharose beads were purchased from GE Healthcare. Human L1 FLAG-tagged, Myc-tagged, and EGFP-tagged constructs were generated by PCR amplification and cloning into pCMV-Tag4 (Stratagene), pEF1/Myc-His A (Invitrogen), and pEGFP-N1 (Clontech), respectively. pCI-neo (Promega) encoding full-length Myc-tagged bovine Rabex-5 and dynamin 1-HA (wild-type and K44A) constructs were generously provided by Dr. J. S. Bonifacino (Eunice Kennedy Shriver National Institute of Child Health and Human Development, National Institutes of Health) and Dr. S. L. Schmid (The Scripps Research Institute, La Jolla, CA), respectively. The human Rab5a construct was PCR-amplified from cDNA and subcloned into an EGFP-N1 vector. Mouse ezrin Myc-tagged construct was generated by PCR amplification and cloning into pEF1/Myc-His A. L1 FLAG-tagged mutants, GFP-Rab5 mutants, and Myc-tagged Rabex-5 mutants were generated using the QuikChange Site-Directed Mutagenesis kit (Stratagene), according to the manufacturer's instructions, and primers containing the corresponding mutant sequences. All constructs were confirmed by DNA sequencing. The custom-designed siRNA duplex for Rabex-5 (821–839, target sequence 5-CAGATATCATTGAGATGGA-3) was obtained from Sigma-Aldrich. Scrambled siRNAs for Rabex-5 were used as negative controls.

Cell Culture and cDNA Transfection—Mouse neuroblastoma N2a cells and human embryonic kidney 293T (HEK293T) cells were maintained in DMEM supplemented with 10% heat-inactivated fetal bovine serum (FBS). Plasmid DNA was transfected into cells by using Lipofectamine 2000 (Invitrogen).

Immunoprecipitation—N2a cells were incubated with anti-L1 polyclonal antibody or anti-mouse L1 monoclonal antibody (5 μg/10^6 cells) for 30 min on ice. After washing unbound antibodies, cells were lysed for 60 min on ice in lysis buffer (1% Triton X-100, 50 mM Tris-HCl, pH 7.4, 150 mM NaCl, 5 mM EDTA, 5 mM EGTA, 10 mM *N*-ethylmaleimide) containing aprotinin, benzamide, and leupeptin protease inhibitors to examine interactions between Rabex-5 and L1 and/or Rab5. To confirm ubiquitination of L1, cells were lysed in radioimmunoprecipitation assay buffer (1% sodium deoxycholate, 0.1% SDS, 1% Triton X-100, 50 mM Tris-HCl, pH 7.4, 150 mM NaCl, 5 mM EDTA, 5 mM EGTA, 10 mM *N*-ethylmaleimide, and protease inhibitors described above) and/or in denaturing buffer (1% SDS, 1% Triton X-100, 50 mM Tris-HCl, pH 7.4, 150 mM NaCl, 5 mM EDTA, 5 mM EGTA, 10 mM *N*-ethylmaleimide, and protease inhibitors described above). Lysates were clarified by centrifugation at 15,000 $\times$ *g* for 20 min. Soluble extracts were incubated with goat anti-L1, anti-Myc, or anti-FLAG antibodies for 5 h, and then protein G-Sepharose beads were added and incubated for a further 1 h. Immunoprecipitated complexes were washed six times with lysis buffer, and bound proteins were eluted with SDS sample buffer.

Immunoblot Analysis—Samples were boiled for 5 min, electrophoresed on NuPage 3–8% Tris acetate gels (Invitrogen), and transferred electrophoretically to PVDF membranes. After blocking nonspecific binding sites, PVDF membranes were probed with antibodies diluted in 20 mM Tris-HCl, pH 7.8, and 150 mM NaCl containing 0.05% Tween 20. After extensive washing, immunoreactivity was detected using an enhanced chemiluminescence detection kit (Pierce).

Subcellular Fractionation—Cells were rinsed with ice-cold PBS and scraped into fractionation buffer (100 mM Tris-HCl, pH 7.4, containing protease inhibitors). Cells were then homogenized using a Dounce homogenizer and centrifuged at 850 $\times$ *g* for 10 min to remove nuclei and cell debris, and post-nuclear supernatants were subjected to ultracentrifugation at 200,000 $\times$ *g* for 10 min in a Himac CS120GXL centrifuge (Hitachi, Tokyo, Japan) to separate the membrane (pellet) and cytosolic (supernatant) fractions. The pellet was resuspended in fractionation buffer. Proteins in each fraction (50 μg/μl) were analyzed by SDS-PAGE and immunoblot assay, as described above.

Biotinylation Assay for Endocytosis—Cells pretreated with cycloheximide (CHX; 10 μg/ml) and leupeptin (0.3 mM) were washed with ice-cold PBS and biotinylated by incubating with 300 μg/ml EZ-Link-Sulfo-NHS-SS-Biotin (Pierce) for 30 min at 4 °C. Excess biotin was quenched by washing with DMEM. Following this, DMEM at 37 °C was added, and biotinylated cells were treated with polyclonal L1-Ab for the indicated times. Remaining cell surface biotin was stripped using stripping solution (50 mM glutathione, 0.3 M NaCl, 75 mM NaOH, and 1% FBS). Cell extracts were made, and cell debris was removed by centrifugation at 14,000 $\times$ *g* for 20 min. Clarified cell extracts were precipitated using streptavidin and immobilized on agarose beads at 4 °C for 2 h. After washing five times with cell lysis buffer, the bound proteins were removed with SDS sample buffer.

Imaging and Quantification—After transfection (48 h), cells were rinsed with PBS, fixed in 4% formaldehyde for 30 min, and permeabilized with 0.3% Triton-X in PBS for 30 min. Primary antibodies were diluted in PBS containing 10% FBS. Labeled cells were visualized using a 1X71 fluorescence microscope (Olympus, Tokyo, Japan) with a 60× oil immersion objective lens. Quantification of surface and/or intracellular fluorescence intensities of L1 was done with MetaMorph imaging software (Universal Imaging Corp.) using an arbitrary threshold. To examine colocalization of fluorescence signals in different channels, the MetaMorph colocalization function following background subtraction and threshold setting were used. Laser-scanning confocal microscopy was performed using an Olympus FV-1000 equipped with a 63× oil immersion objective lens. In at least three independent experiments, 30 cells were photographed and analyzed for each construct. Statistical analysis was done using ANOVA and post hoc tests with appropriate Bonferroni adjustment for multiple comparisons, to ensure a significance level of 0.05 in all experiments. *, **, and *** represent <0.05, <0.01, and <0.001, respectively. *Error bars* denote the S.E.

RESULTS

L1 Undergoes Ubiquitination and Lysosomal Degradation following Incubation with L1-Ab—Previous studies on L1 demonstrated that cell adhesion can be spatially regulated by the polarized internalization and recycling of cell adhesion molecules (3, 4). Indeed, time lapse imaging directly showed that internalization of L1-GFP localized on the plasma membrane into intracellular vesicles depends on cell adhesion in N2a cells (Fig. 1*A*, *arrows*). To gain insight into the molecular machinery underlying cell adhesion-dependent internalization and postendocytic sorting of L1, I investigated L1 endocytosis induced by incubation with L1-Ab, which mimics L1-L1 homophilic binding (9, 24) in N2a cells. Immunocytochemical analysis showed that endogenous L1 was localized predominantly to the plasma membrane in untreated cells (95.5% $\pm$ 1.2%; $n = 3$), with a small amount present in intracellular vesicles (4.5% $\pm$ 0.9%; $n = 3$) (Fig. 1*B*, *left panel*). In cells pretreated with L1-Ab at 4 °C and then incubated at 37 °C, L1 was redistributed from the plasma membrane into intracellular vesicles (Fig. 1*B*, *arrows*); this finding was consistent with those of previous reports (9, 24). The percentage of intracellular to total fluorescence intensity of L1 increased with an increase in the L1-Ab incubation time, *i.e.* 15.5% $\pm$ 1.5% after 10 min ($n = 3$), 27.5% $\pm$ 1.7% after 20 min ($n = 3$), and 32.2% $\pm$ 1.2% after 30 min ($n = 3$). Colocalization of endocytic/degradative compartment proteins was investigated to identify the intracellular vesicle structures containing L1. Image quantification confirmed that 4.6% $\pm$ 1.2%, 4.5% $\pm$ 1.1%, and 4.7% $\pm$ 1.1% ($n = 3$) of L1 colocalized with the Rab5 early endosome marker, the Rab11 marker for recycling endosomes (data not shown), and the LysoTracker lysosomal marker (Fig. 2*A*, *lower left panels*), respectively, in untreated cells. In contrast, L1 colocalization with Rab5, Rab11, and LysoTracker significantly increased to 12.2% $\pm$ 1.5%, 15.6% $\pm$ 1.2%, and 18.7% $\pm$ 1.5% ($n = 3$), respectively, upon incubation with L1-Ab (Fig. 2*A*, *arrows*). These data indicate that L1-L1 homophilic binding leads to L1 internalization and sorting into recycling endosomes for recycling and/or lysosomes for degradation via Rab5-positive early endosomes.

Next, I asked whether L1-Ab-dependent internalization of L1 is involved in triggering posttranslational modification of L1, such as dephosphorylation of the tyrosine-based motif (9) and ubiquitination which is critical role in sorting of NCAM, DM-GRASP, and L1 (25–27). Consistent with previous results (9, 25), L1-Ab treatment led to L1 monoubiquitination (Fig. 2*B*, *left panel*) and a -fold increase in dephosphorylation of the tyrosine-based motif in L1 of 1.8 $\pm$ 0.2 (Fig. 2*C*, *left panel*, *lane 1 versus lane 2*, $n = 3$, $p < 0.01$). Furthermore, weak but detectable bands were observed upon L1-Ab treatment with FK1 antibody that recognizes polyubiquitination (Fig. 2*B*, *right panel*), indicating that L1-bound ubiquitin contained both monoubiquitin and polyubiquitin chains.

To examine whether phosphorylation of the tyrosine-based motif is controlled by the Src kinase, as reported previously (9), the cells were pretreated with the Src kinase inhibitor PP2 and then incubated with L1-Ab. As expected, dephosphorylation of the L1 tyrosine-based motif in PP2-pretreated cells significantly increased by 1.5 $\pm$ 0.1-fold compared with control cells (Fig. 2*C*, *left panel*, *lane 2 versus lane 4*, $n = 3$, $p < 0.01$). Surprisingly, the extent of L1 ubiquitination in PP2-pretreated cells significantly increased by 1.4 $\pm$ 0.2-fold (Fig. 2*C*, *right panel*, *lane 4 versus lane 2*, $n = 3$, $p < 0.01$), indicating a possible involvement of the Src kinase in regulating L1 ubiquitination. Although the apparent dependence of endocytosis on ubiquitination suggests an early role for the ubiquitination process in internalization, it is possible that L1 ubiquitination occurs after internalization and that its role may instead be to prevent receptor recycling to the plasma membrane from an internalized pool. To address this question, I inhibited the progression of endocytosis by expressing dominant negative dynamin, namely dynamin^{K44A} (28). Expression of dynamin^{K44A} drastically inhibited L1 internalization after L1-Ab incubation compared with control cells (Fig. 2*D*, *middle panels*). Importantly, compared with the nontransfected cells, L1 ubiquitination in cells expressing dynamin^{K44A} significantly increased before and after L1-Ab incubation by 2.2 $\pm$ 0.4-fold (Fig. 2*D*, *lower panels*, *lane 3 versus lane 1*, $n = 3$, $p < 0.01$) and 1.4 $\pm$ 0.2-fold (Fig. 2*D*, *lower panels*, *lane 4 versus lane 2*, $n = 3$, $p < 0.01$), respectively, suggesting that ubiquitination occurs before internalization from the plasma membrane.

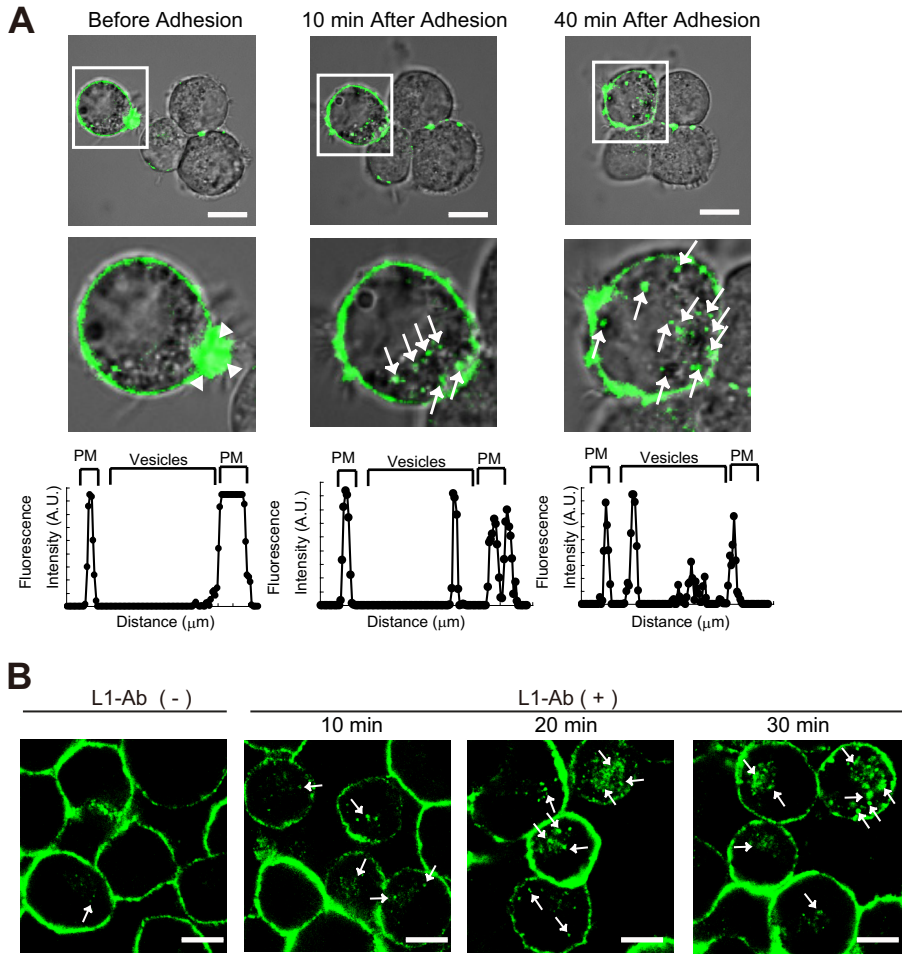

FIGURE 1. **L1 ligand-dependent internalization of L1 in N2a cells.** *A*, time-lapse imaging showing cell adhesion-dependent internalization of L1-GFP (*arrows*) in N2a cells (*upper panels*). Note that L1-GFP accumulates on the lamellipodium tip before the cells adhere to each other (*arrowheads*). *White boxed* areas are enlarged (*middle panels*). *Scale bars* represent 10 μm. A representative density profile plot was generated using SCION Image software (*lower panels*). Pixel intensity was determined by a row average plot of a section selected from a confocal slice through the center of the cell. *PM*, plasma membrane. *B*, L1-Ab-induced endocytosis of L1 in N2a cells. Live cells were incubated with L1-Ab at 4 °C and then incubated for the indicated time periods at 37 °C. Note that a few cells that are in contact show intracellular L1-GFP before L1-Ab-induced endocytosis (*left panel*). N2a cells were labeled with Alexa Fluor 488-conjugated L1 antibodies (*green*). *Arrows* indicate internalized L1. *Scale bars* represent 10 μm.

To address the relationship between L1 ubiquitination and protein degradation, I measured the metabolic stability of endogenous L1 by immunoblotting following inhibition of protein synthesis with CHX. In the presence of L1-Ab, L1 had a significantly faster turnover rate than that in the absence of L1-Ab, its half-life being 4.3 h and 1.9 h in the absence and presence of L1-Ab, respectively (Fig. 2*E*). The accelerated degradation of L1 in the presence of L1-Ab can at least in part be attributed to lysosomal proteolysis because preventing lysosomal acidification and delivery by using bafilomycin A1, a vacuolar H^+-ATPase inhibitor, significantly delayed L1 degradation (Fig. 2*E*). On the contrary, the cysteine protease and proteasomal inhibitor lactacystin partially stabilized L1 (Fig. 2*E*). Overall, these results suggest that L1 is subjected to both mono- and polyubiquitination on the plasma membrane and is sorted into lysosomes, but not proteasomes, via Rab5 early endocytic trafficking pathway upon L1-L1 homophilic binding.

Ubiquitination Plays an Important Role in L1 Internalization and Targeting to Lysosomal Compartments—To establish the role of L1 Ub modification on internalization and traffic to the lysosome, I constructed a ubiquitination-deficient mutant of L1, $L1^{K11R}$, in which a Lys is replaced with Arg at position 11 in the cytoplasmic tail (Fig. 3*A*). The intracellular domain of L1 contains 11 Lys residues, two of which form a putative ezrin-binding motif (29) (Fig. 3*A*). As expected, ubiquitination of $L1^{K11R}$ mutants was drastically reduced by 80–90% compared with $L1^{WT}$ (Fig. 3*B*). Intriguingly, Myc-tagged ezrin did not coimmunoprecipitate with FLAG-tagged L1 in the cells overexpressing HA-tagged Ub (Fig. 3*C*) but did in control cells, providing the possibility that ubiquitination within the L1 ezrin-binding site interferes with ezrin binding because of steric hindrance by ubiquitination.

Next, I compared the kinetics of internalization of surface-biotinylated $L1^{WT}$ and $L1^{K11R}$ in cells preincubated with CHX to determine the role of L1 ubiquitination in internalization (Fig. 3*D*). Surface-biotinylated L1 was internalized after 15 min in untreated cells (15.8% ± 1.4%; $n = 3$), indicating that L1 undergoes constitutive endocytosis from the plasma membrane (Fig. 3*D*). Notably, L1-Ab-dependent $L1^{WT}$ internalization peaked after 15 min (39.8% ± 4.4%; $n = 3$), whereas the rate of L1-Ab-dependent $L1^{K11R}$ internalization was similar to the

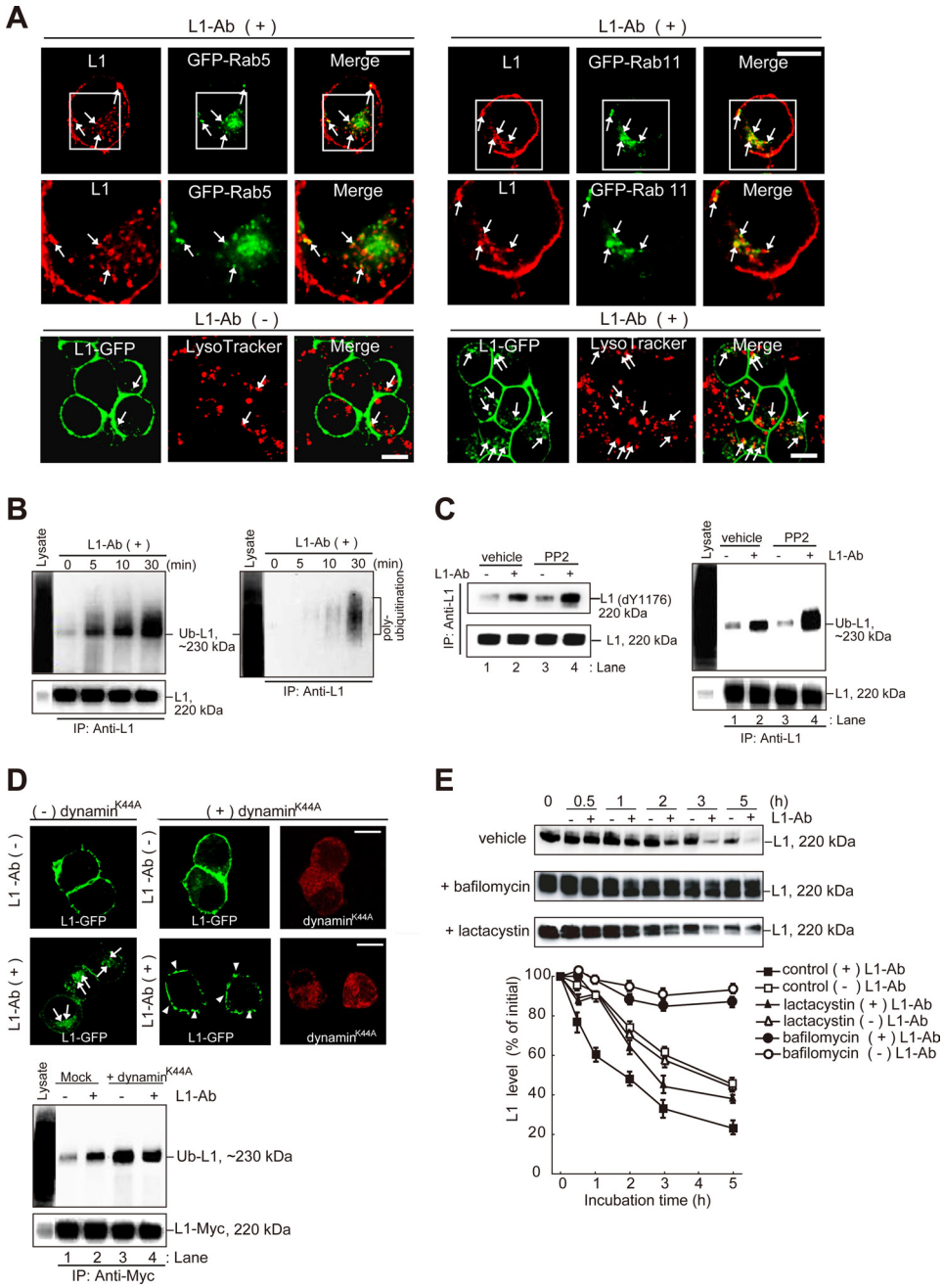

FIGURE 2. **Ubiquitination, lysosomal targeting, and degradation of L1 after incubation with L1-Ab.** *A*, superimposed images show the colocalization of internalized L1 (*red*) and GFP-Rab5 (*green*)-positive early endosomes or GFP-Rab 11 (*green*)-positive recycling endosomes (*upper panels*). *White boxed areas* are enlarged (*middle panels*). *Arrows* indicate the L1 colocalization with Rab5- or Rab11-positive vesicles. Colocalization of L1-GFP with LysoTracker Red DND-99 is shown in *lower panels*. Lysosomes are shown in *red*, and colocalized components are shown *yellow* (*arrows*). Note that a few cells that are in contact show the colocalization of intracellular L1-GFP with LysoTracker Red DND-99 before L1-Ab-induced endocytosis (*lower left panels*). *Scale bars* represent 10 μm. *B*, N2a cells were incubated in the presence of L1-Ab. After cell lysis, immunoprecipitation (*IP*) and immunoblot analyses were performed as indicated. The blots were stripped and reprobed with anti-FK1 antibody that recognizes polyubiquitination (*right panel*). To control the functionality of the antibodies cell lysates were applied (*Lysate*). *C*, N2a cells treated with PP2 were incubated in the presence or absence of L1-Ab. After cell lysis, immunoprecipitation and immunoblot analyses were performed. Dephosphorylation (*dY1176*) of tyrosine 1176 (*Y1176*) in the YRSL motif within the cytoplasmic domain of L1 was detected using the 74-5H7 monoclonal antibody (9) (*left panel*). *D*, N2a cells co-expressing L1-GFP (*green*) with or without the dynamin^{K44A} mutant (*red*) were incubated in the absence (*upper panels*) or presence (*middle panels*) of L1-Ab. *Arrows* and *arrowheads* indicate internalized L1 and accumulated L1 on plasma membrane, respectively (*middle panels*). *Scale bars* represent 10 μm. N2a cells coexpressing the indicated plasmids were incubated in the presence or absence of L1-Ab. After cell lysis, immunoprecipitation and immunoblot analyses were performed (*lower*). *E*, metabolic stability of endogenous L1 in N2a cells was measured in the presence of bafilomycin A1 (1 μM) or lactacystin (10 μM) after inhibiting translation with 10 μg/ml CHX. Equal amounts of cell lysates were immunoblotted with L1-Ab (*upper*). Degradation kinetics of L1 were determined by densitometry of immunoblots illustrated in the *upper panels* (*lower*). Data are displayed as the mean ± S.E. (*error bars*) of triplicate experiments.

rate of L1-Ab-independent L1^{WT} internalization (16.2% ± 1.2%; $n = 3$), suggesting that ubiquitination of L1 is required to obtain the maximal internalization rate.

Because the cytoplasmic domain of L1 is known to contain a tyrosine-based sorting motif, I constructed a single amino acid substitution of Tyr^{1176} to Ala within this motif to compare the

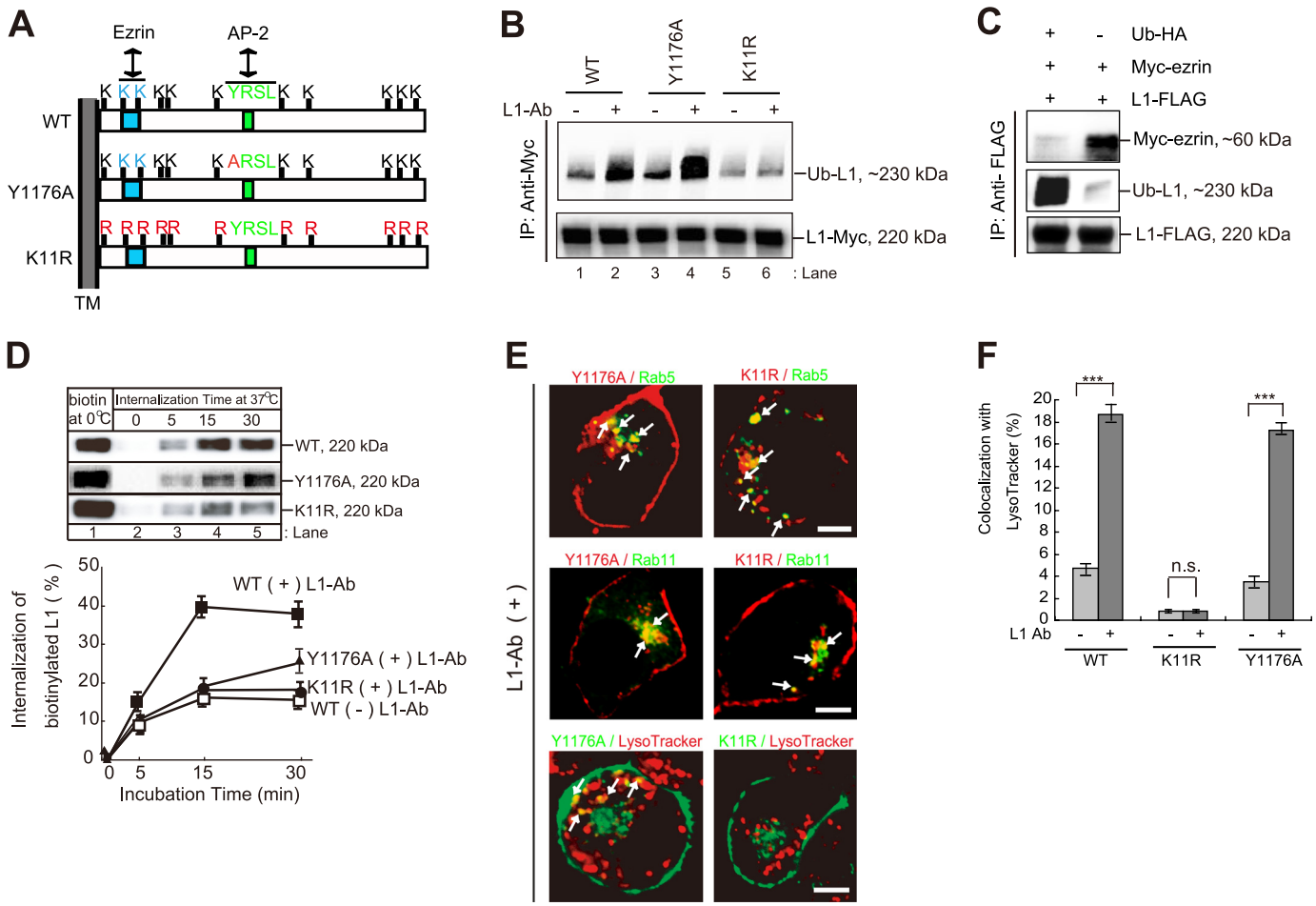

FIGURE 3. **Characterization of L1^{K11R} and L1^{Y1176A} mutants.** *A*, schematic diagram shows the cytoplasmic domain structure of human L1. *Light blue*, putative ezrin-binding motif (KGGK); *light green*, tyrosine-based AP-2 binding motif (YRSL). *Red characters* indicate the sites of point mutations used in this study. *TM*, transmembrane. *B*, N2a cells expressing the indicated plasmids were incubated in the presence or absence of L1-Ab. After cell lysis, immunoprecipitation (*IP*) and immunoblot analyses were performed as indicated. *C*, after N2a cells coexpressing the indicated plasmids lysis, immunoprecipitation and immunoblot analyses were performed. *D*, CHX-treated cells were surface-biotinylated at 0 °C (*lane 1*) and then incubated at 37 °C for periods of 0–30 min (*lanes 2–5*). Surface-biotinylated proteins were recovered with streptavidin-agarose from cell extracts and analyzed by immunoblotting (*upper*). Relative amounts of internalized biotinylated L1^{WT}, L1^{Y1176A}, and L1^{K11R} FLAG-tagged were measured by densitometry and expressed as a percentage of the total initial surface biotinylated pool (*lower*). Data are displayed as the mean ± S.E. (*error bars*) of triplicate experiments. *E*, Myc-L1^{Y1176A} or Myc-L1^{K11R} (*red*; *upper* and *middle panels*) was colocalized with GFP-Rab5- and GFP-Rab11-positive endosomal compartments in the presence of L1-Ab (*green*; *upper* and *middle panels*). L1^{Y1176A}-GFP or L1^{K11R}-GFP (*green*) was colocalized with LysoTracker Red DND-99 (*red*; *bottom panels*). *Arrows* indicate the colocalization (*yellow*). *Scale bars* represent 5 μm. F, colocalization of L1^{WT}-GFP, L1^{Y1176A}-GFP, and L1^{K11R}-GFP with LysoTracker was quantified, and the percentage colocalization was plotted for each. Data are displayed as the mean ± S.E. (*error bars*). ***, $p < 0.001$; *n.s.*, not significant.

rate of internalization of this mutant with L1^{K11R}. Consistent with the enhancement of L1 ubiquitination by PP2 (Fig. 2*C*, *right panel*), the extent of L1^{Y1176A} ubiquitination significantly increased by 1.3 ± 0.1-fold compared with the L1^{WT} (Fig. 3*B*, *lane 4 versus lane 2*, $n = 3$, $p < 0.01$), suggesting that dephosphorylation at the tyrosine-based motif plays a critical role in the ubiquitination of L1. However, its internalization is grossly retarded after 15-min incubation (16.8% ± 2.4%) and only slightly greater than that of L1^{K11R} after 30 min (Fig. 3*D*). These results confirm that ubiquitination is not sufficient for rapid L1 internalization and turnover and suggest that the endocytic motif also plays a key role in this process. I next examined whether L1^{Y1176A} and L1^{K11R} are targeted to the endosomes and lysosomal compartments after internalization. L1^{Y1176A} was detected on Rab5- and Rab11-positive endosomes and LysoTracker-positive lysosomes upon L1-Ab incubation (Fig. 3*E*, *arrows*). Although L1^{K11R} was also present on Rab5- and Rab11-positive endosomes, only a little L1^{K11R} was detected on LysoTracker-positive lysosomes in the presence of L1-Ab. Image quantification revealed that colocalization of L1^{WT}, L1^{K11R}, and L1^{Y1176A} with lysosomes was 18.7% ± 1.5%, 0.8% ± 0.1%, and 17.2% ± 1.1%, respectively (Fig. 3*F*), suggesting that ubiquitination is required for the L1 protein to be internalized and targeted for lysosomal degradation.

Rabex-5 Interacts Directly with Ubiquitinated L1 via MIU—As extensive colocalization of endogenous L1 and Rab5 was observed following L1-Ab incubation (Fig. 2*A*), I next sought to determine whether Rab5 is involved in L1 internalization by expressing wild-type Rab5, or GTPase-deficient Rab5^{Q79L}, or GTP-binding-deficient Rab5^{S34N} mutants in N2a cells. The Rab5^{S34N} dominant negative GFP-Rab5 mutant (30) did not affect endogenous L1 distribution (Fig. 4*A*). However, endogenous L1 was significantly redistributed from the plasma membrane to enlarged vacuoles by the expression of the constitutively

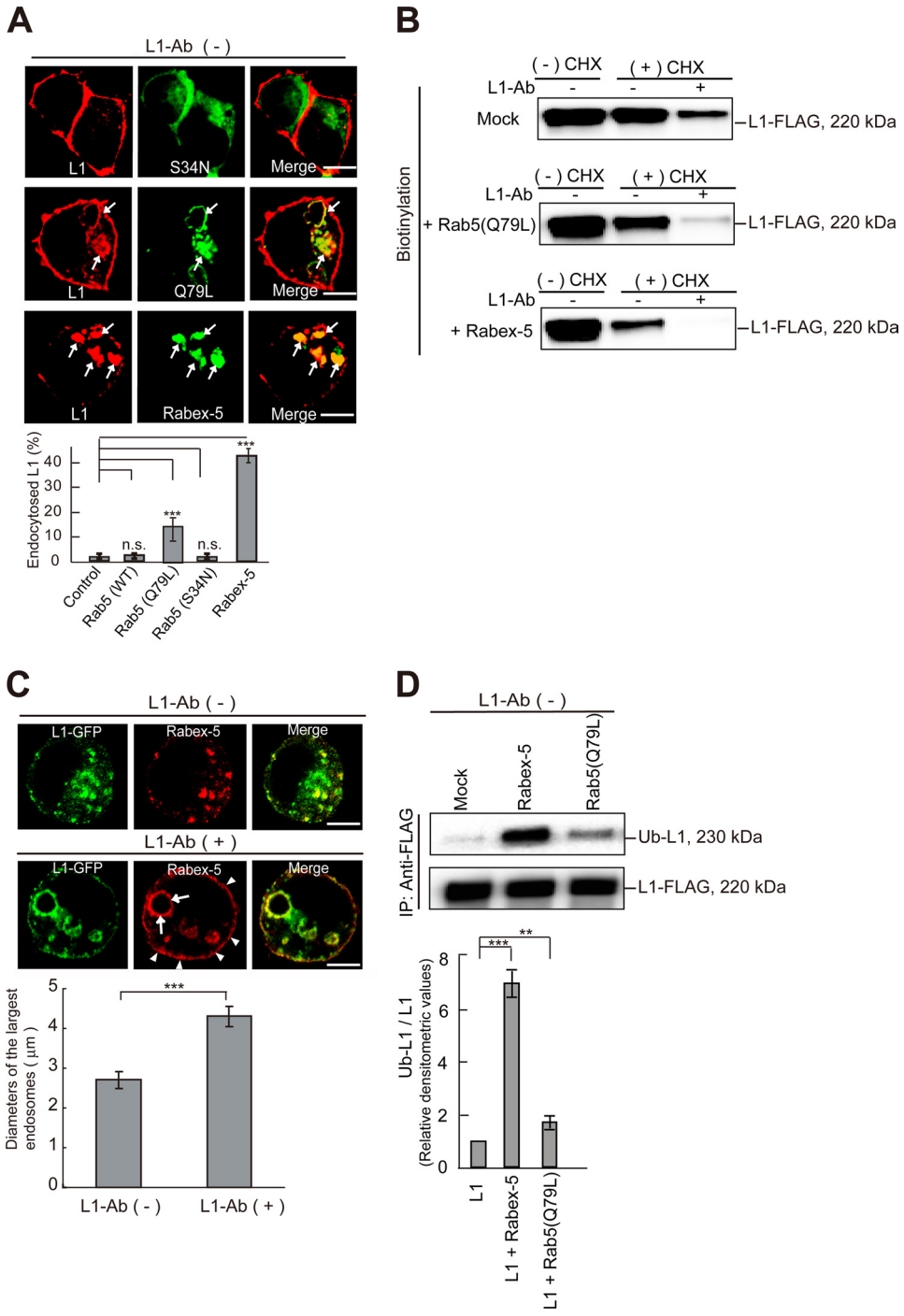

FIGURE 4. **Impact of the expression of Rab5 mutants and Rabex-5 on L1 subcellular distribution.** *A*, colocalization of endogenous L1 with GFP-Rab5 mutants and Myc-tagged Rabex-5 in N2a cells (*upper*) is shown. *Arrows* indicate internalized L1 in $Rab5^{Q79L}$- and Rabex-5-positive endosomes. *Scale bars* represent 5 μm. Fluorescence intensities were quantified, and the percentage of perinuclear to total fluorescence was plotted (*lower*). Data are displayed as the mean ± S.E. (*error bars*). ***, $p < 0.001$; *n.s.*, not significant. *B*, CHX-nontreated cells (−*CHX*) or CHX-treated cells (+*CHX*) expressing the indicated plasmids were surface-biotinylated. Cells were then incubated in the presence or absence of L1-Ab. Surface-biotinylated proteins were recovered with streptavidin-agarose from cell extracts and analyzed by immunoblotting. *C*, N2a cells expressing L1-GFP (*green*) and Myc-tagged Rabex-5 (*red*) were incubated in the absence (*upper panels*) or presence (*middle panels*) of L1-Ab. *Arrowheads* and *arrows* indicate plasma membrane-targeted Rabex-5 and Rabex-5-induced enlarged endosomes, respectively. *Scale bars* represent 5 μm. The diameters of the largest Rabex-5-labeled endosomes in 30 cells expressing Myc-tagged Rabex-5 were measured; the graph shows the mean ± S.E. (*lower*). ***, $p < 0.001$. *D*, N2a cells were transfected with the indicated plasmids. Accumulation of monoubiquitinated L1 was examined by immunoprecipitation and analyzed by immunoblotting (*upper*). *Bars* represent the relative densitometric values of Ub-L1/L1 (*lower*). Data are displayed as the mean ± S.E. ***, $p < 0.001$; **, $p < 0.01$.

active $Rab5^{Q79L}$ mutant (30) in the absence of L1-Ab (Fig. 4*A*, *arrows*), and redistribution was further enhanced in the presence of L1-Ab (data not shown). The impact of $Rab5^{Q79L}$ on L1 redistribution is similar to its enhancement of the intracellular distribution of the EGF and m4 muscarinic acetylcholine receptors (31, 32). Intriguingly, enhanced L1 redistribution in the cells expressing Myc-tagged Rabex-5 was greater than in the cells expressing the GFP-$Rab5^{Q79L}$ mutant (Fig. 4*A*).

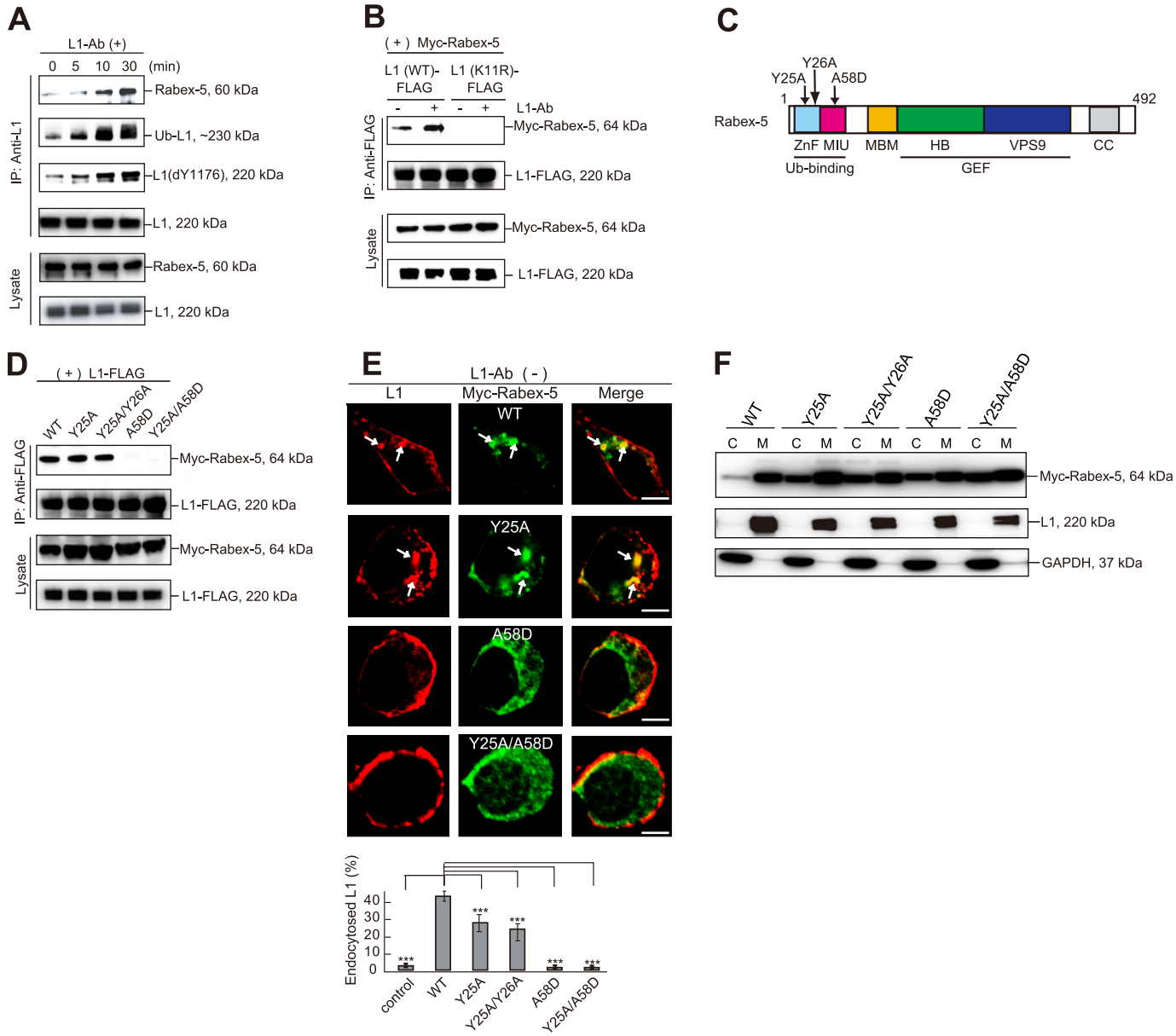

FIGURE 5. **Direct interaction of Rabex-5 with ubiquitinated L1 occurs via MIU, but not ZnF.** *A*, N2a cells were incubated with L1-Ab for the indicated times. All samples were immunoprecipitated with goat L1-Ab and analyzed by immunoblotting. *B*, N2a cells coexpressing the indicated plasmids were incubated in the presence or absence of L1-Ab. After cell lysis, immunoprecipitation and immunoblot analyses were performed. *C*, schematic diagram shows the domain structure of bovine Rabex-5. *Light blue*, ZnF; *magenta*, MIU; *orange*, membrane-binding motif; *green*, helical bundle (*HB*); *blue*, VPS9; *gray*, coiled coil (*CC*) domain. *Arrows* indicate the Rabex-5 mutants used in this study. *D*, cells coexpressing L1 FLAG-tagged with the indicated Myc-tagged Rabex-5 mutants were immunoprecipitated (*IP*) and analyzed by immunoblotting. *E*, N2a cells transfected with the indicated plasmids were stained with L1 (*red*) and Myc (*green*) antibodies (*upper*). *Arrows* indicate L1 accumulation on Rabex-5-positive endosomes. *Scale bars* represent 5 μm. Fluorescence intensities were quantified, and the percentage of perinuclear to total fluorescence was plotted (*lower*). ***, $p < 0.001$. *F*, immunoblotting shows membrane and cytosolic distributions in N2a cells expressing the indicated plasmids, endogenous L1 and GAPDH. *C*, cytosol; *M*, membrane.

Given that the GTP-bound activated form of Rab5 promotes L1 internalization, I measured the amount of cell surface biotinylated L1 in cells expressing $Rab5^{Q79L}$ or Rabex-5 before and after L1-Ab incubation. As expected, there was significantly less biotinylated L1 on the surface of cells expressing $Rab5^{Q79L}$ and a further reduction in cells expressing Rabex-5 before and after L1-Ab incubation (Fig. 4*B*). Furthermore, Rabex-5 was translocated to the plasma membrane (Fig. 4*C*, *middle panels*) and enlarged endosomal compartments upon incubation with L1-Ab (Fig. 4 C, *lower panel*). Taken together, these data suggest that L1-Ab clustering leads to Rab5 GEF activation via Rabex-5 recruitment to the plasma membrane to accelerate the internalization of L1. Surprisingly, the amount of ubiquitinated L1 was dramatically increased by 6.8 ± 0.9-fold in cells expressing Rabex-5 compared with the untransfected cells (Fig. 4*D*). However, these results raised the question of why prolonged Rabex-5 expression should cause significant L1 redistribution from the plasma membrane into the endosomes.

Because L1 is ubiquitinated and Rabex-5 contains UBDs, I next examined whether Rabex-5 causes ubiquitinated L1 to accumulate through a direct interaction. Rabex-5 was found to coimmunoprecipitate with L1 in untreated cells, and this was

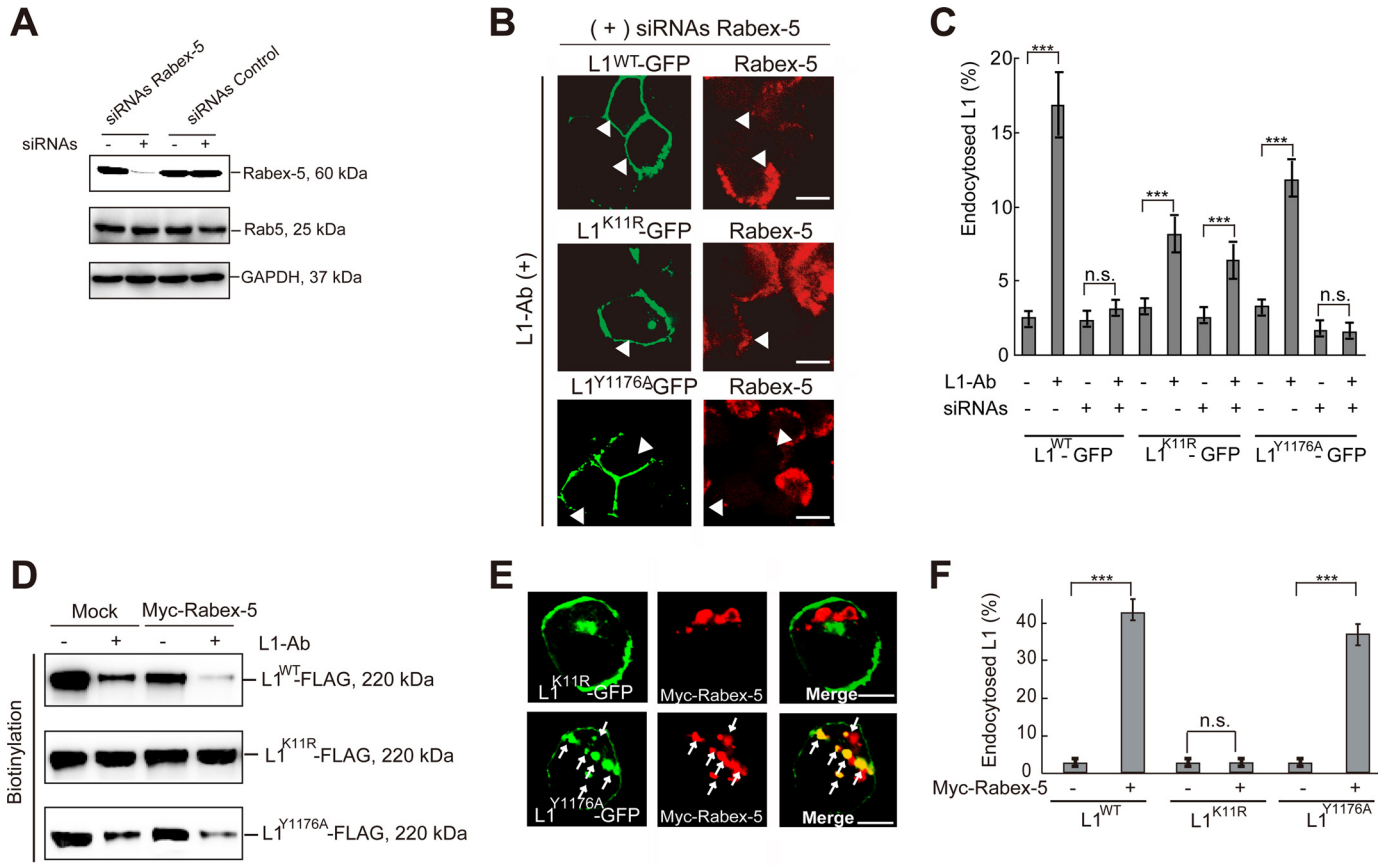

FIGURE 6. **Impact of Rabex-5 siRNAs-mediated knockdown or overexpression on L1 endocytosis.** *A*, lysates of cells treated with Rabex-5 siRNAs or negative control siRNAs were analyzed by immunoblotting. *B*, cells cotransfected with Rabex-5 siRNAs and the indicated plasmids were incubated with L1-Ab, followed by immunocytochemistry. *Arrowheads* indicate Rabex-5-depleted cells. *Scale bars* represent 10 μm. *C*, fluorescence intensities of $L1^{WT}$-GFP, $L1^{K11R}$-GFP, and $L1^{Y1176A}$-GFP were quantified, and the percentage of perinuclear to total fluorescence was plotted. Data are presented as the mean ± S.E. (*error bars*) of triplicate experiments. ***, $p < 0.001$; *n.s.*, not significant. *D*, N2a cells pretreated with CHX co-expressing of Myc-tagged Rabex-5 with indicated plasmids were surface-biotinylated on ice. Surface-biotinylated proteins were recovered with streptavidin-agarose from cell extracts and analyzed by immunoblotting. *E*, colocalization of Myc-tagged Rabex-5 (*red*) with $L1^{K11R}$-GFP (*green*) (*upper panels*) or $L1^{Y1176A}$-GFP (*green*) (*lower panels*). *Scale bars* represent 5 μm. *F*, fluorescence intensities were quantified, and the percentage of perinuclear to total fluorescence was plotted. ***, $p < 0.001$; *n.s.*, not significant.

enhanced by incubation with L1-Ab (Fig. 5*A*). To examine further whether Rabex-5 association with L1 depends on the L1 ubiquitination status, a coimmunoprecipitation study was conducted using wild-type and mutant L1. Although Rabex-5 strongly associated with $L1^{WT}$, no interaction was observed with the $L1^{K11R}$ ubiquitination-deficient mutant (Fig. 5*B*), suggesting that Rabex-5 association with L1 is governed principally by the ubiquitination state of L1.

Because Rabex-5 contains two independent UBDs in the N terminus (18, 19), I next examined which of these domains mediates the interaction with ubiquitinated L1. For this, I constructed the Rabex-$5^{Y25A/A58D}$ double mutant, mutated in the both the A20 ZnF and MIU domains, and the respective single mutants (Fig. 5*D*). Rabex-5^{Y25A}, but not Rabex-5^{A58D} or Rabex-$5^{Y25A/A58D}$ proteins, coimmunoprecipitated with L1 (Fig. 5*D*), suggesting that the MIU domain is critical for Rabex-5 association with ubiquitinated L1. Although the A20 ZnF domain exhibits Ub-ligase activity (18, 19), knockdown of Rabex-5 with siRNAs did not affect the level of L1 ubiquitination relative to the controls either before or after L1-Ab stimulation (data not shown), indicating that L1 is not a substrate for Rabex-5 Ub-ligase activity. Consistent with a previous report that membrane targeting of Rabex-5 is mediated by the association of Rabex-5 UBDs with ubiquitinated membrane proteins (33), all three Rabex-5 mutants redistributed from the membrane to the cytosolic fraction (Fig. 5, *E* and *F*).

To further establish differences in the functional properties between these UBDs, I compared the amounts of internalized L1 in cells expressing Rabex-5 mutants (Fig. 5*E*). Rabex-5^{WT} or Rabex-5^{Y25A} expression redistributed L1 from the plasma membrane to the endosomes even in the absence of L1-Ab (Fig. 5*E*, *arrows*), causing an accumulation of the ubiquitinated L1. In contrast, Rabex-5^{A58D} and the Rabex-$5^{Y25A/A58D}$ double mutant had no effect on L1 distribution (Fig. 5*E*). These results suggest that the MIU domain, but not A20 ZnF, plays an important role in L1 internalization through direct interaction with ubiquitinated L1.

Modulation of Rabex-5 Expression Regulates the Plasma Membrane Pool of L1—To demonstrate directly the functional role of Rabex-5 in L1 endocytosis, endocytosis of $L1^{WT}$, $L1^{Y1176A}$, and $L1^{K11R}$ was measured in cells depleted of Rabex-5 by Rabex-5 siRNAs. Rabex-5 siRNAs largely eliminated Rabex-5 expression (Fig. 6*A*). Notably, no punctuate structures containing $L1^{WT}$-GFP or $L1^{Y1176A}$-GFP were observed in Rabex-5-depleted cells following L1-Ab incubation (Fig. 6*B*). Indeed, quantitative analysis confirmed that endocytosis of

$L1^{WT}$ and $L1^{Y1176A}$ was impaired in Rabex-5-depleted cells treated with L1-Ab (Fig. 6*C*). In contrast, $L1^{K11R}$-GFP internalization was not affected by Rabex-5 depletion despite there being significantly lower $L1^{K11R}$ endocytosis compared with $L1^{WT}$ (~55% ± 5%; Fig. 6*C*). Conversely, a biotinylation assay and immunofluorescence analysis revealed that Rabex-5 overexpression promoted a dramatic down-regulation of cell surface $L1^{WT}$ and $L1^{Y1176A}$, but not of $L1^{K11R}$ (Fig. 6*D*), leading to the accumulation of $L1^{WT}$ and $L1^{Y1176A}$, but not $L1^{K11R}$, on Rabex-5-positive endosomes (Fig. 6, *E* and *F*). These results strongly suggest that the association of ubiquitinated L1 with Rabex-5 MIU on the plasma membrane promotes efficient internalization and proper postendocytic trafficking to lysosomes.

DISCUSSION

Both activation and attenuation of the L1 signal are tightly regulated by endocytosis. Therefore, elucidating the regulation of cell surface L1 is important for understanding the molecular mechanisms that underlie many physiological processes involved in central nervous system development. However, the molecular machinery underlying the L1 endocytic trafficking pathway that regulates the plasma membrane pool of L1 following L1-L1 homophilic binding remains unclear. Here, I report that L1 ubiquitination and dephosphorylation within the tyrosine-based motif mediate its internalization and trafficking to the lysosome in an agonist-dependent manner and that endocytosis and endocytic sorting of L1 are mediated by Rabex-5. Rabex-5 overexpression increases the rate of L1 internalization from the plasma membrane, causing an accumulation of ubiquitinated L1 on endosomes, whereas siRNAs-mediated Rabex-5 knockdown blocks L1 internalization. These results clearly indicate that L1 ubiquitination following ligand binding down-regulates cell surface L1 via the Rabex-5-mediated endocytic trafficking pathway.

Roles of Ubiquitination and the Tyrosine-based Endocytic Motif in L1 Endocytosis—The proper control of cell surface L1 expression is essential for maintaining the structural and functional homeostasis of neuronal cells. Ubiquitination is among the most widely used protein modifications involved in regulating cellular signaling and homeostasis. The detection of L1 polyubiquitination was remarkable in light of the data showing that L1 is degraded by lysosomes via the endocytic pathway, rather than by the proteasome. Recent evidence, however, suggests that multiple mono-Ub or poly-Ub moieties are associated with efficient endocytic cargo recognition (*e.g.* the tropomyosin-regulated kinase A receptor (TrkA), major histocompatibility complex (MHC) class I molecules, interferon (IFN)-α/β receptor 1 (IFNAR1) subunit of the type I IFN receptor, and epidermal growth factor receptor (EGFR) (34–37). The essential role of poly-Ub and multimeric Ub in the rapid internalization of transmembrane proteins suggests that polyvalent interactions are required to overcome the low affinity binding of Ub to the Ub-interacting motif of Ub-binding clathrin adaptors (38, 39). Further experiments are needed to address the Ub configuration requirement for endolysosomal sorting of L1 by Rabex-5 and to identify L1-specific Ub-ligases to elucidate the function of Ub in the regulation of L1 signaling and trafficking.

Remarkably, L1 ubiquitination is required, but not sufficient, for maximal L1 internalization, which also depends on a tyrosine-based sorting motif that recruits AP-2. These data are consistent with the finding that the Src kinase inhibitor PP2 significantly enhances both L1 ubiquitination and dephosphorylation simultaneously. Thus, it is possible that the balance of Src kinase and tyrosine phosphatase activities plays a role in regulating L1 endocytosis by controlling the recruitment of a yet unidentified E3 ligase for L1. The interaction between ubiquitination and the clathrin machinery in regulating endocytosis and protein sorting is well studied in many eukaryotic cell types (40). Ubiquitinated receptors are recruited to clathrin-coated pits via interactions with the epsin and eps15 adaptor proteins (14). In addition, receptor ubiquitination may aid interaction with the AP-2 adaptor protein (36). The roles of epsin and AP-2 in regulating endocytosis of neuronal protein are well characterized (41, 42). However, further experiments are required to investigate whether similar endocytic mechanisms are involved in controlling the maximal rate of L1 internalization following L1-L1 homophilic interaction.

Immunocytochemical and biotinylation studies revealed that the $L1^{Y1176A}$ mutant exhibits a slower rate of internalization and a targeting to the lysosomes via the Rabex-5-mediated endocytic pathway. This raises the question of how the $L1^{Y1176A}$ mutant, which does not interact with AP-2 (9), is able to internalize to the endosomes without using the clathrin-mediated endocytic pathway. Multiple internalization pathways have been associated with the uptake of ubiquitinated proteins from the cell surface. Although EGFR is exclusively internalized by the clathrin-dependent pathway in the presence of low EGF concentrations, EGFR is also internalized by clathrin-independent pathway only when exposed to higher concentrations of EGF (43). It is, therefore, possible that the $L1^{Y1176A}$ mutant, which exclusively depends on ubiquitination, is internalized through a different endocytic route such as the clathrin-independent endocytic trafficking pathway.

Novel Endocytic Trafficking Pathway of Ubiquitinated L1 Is Regulated by Rabex-5—UBPs tether ubiquitinated cargo to components of the endocytic and sorting machinery, thereby enabling receptor internalization and postinternalization sorting. Although L1 is constitutively internalized into the endosomes and/or lysosomes even in the absence of L1-Ab, L1-Ab-induced clustering further stimulates L1 ubiquitination concomitant with Rabex-5 recruitment to the plasma membrane to facilitate the ubiquitinated L1 internalization and sorting into lysosomes. Consistent with this, plasma membrane and early endosomal localization of L1 depend on the level of activated Rab5, as the activation of GEF for Rab5 increases the rate of L1 internalization. Taken together with data showing significant accumulation of ubiquitinated L1 in cells overexpressing Rabex-5, these data strongly support the hypothesis that the multidomain architecture of Rabex-5 allows it to perform dual roles in cargo sorting by Ub binding and ubiquitinated adaptors, and Rab5-dependent internalization. Previous studies using Vps9p, the yeast homolog of Rabex-5, indicate a possible cross-talk between the Ub-binding activity of the Coupling of

Ub conjugation to ER degradation (CUE) domain and GEF activity of the VPS9 domain in the ubiquitinated cargo trafficking pathway (44, 45). Based on these data, I propose the hypothesis that ubiquitinated L1 binding to Rabex-5 triggers Rab5 GEF activation through an allosteric mechanism. Further experiments are required to test this hypothesis.

Differential Roles of Two Independent UBDs in Rabex-5—To date, it remains unclear how Rabex-5 discriminates between its two UBDs, ZnF and MIU, depending on the biological context and how these UBDs cooperate with each other to transmit Ub-dependent signaling. A previous study showed that Rabex-5 binding to ubiquitinated EGF receptor in EGF-stimulated cells is dependent on both UBDs. Mutation of either domain alone had little impact on EGF receptor association, whereas mutation of both abolished the EGF receptor interaction (46). Here, I provide the first direct evidence that MIU, but not ZnF, binds and transports ubiquitinated cargo from the plasma membrane. Furthermore, the impact of the MIU domain on L1 internalization is significantly greater than the ZnF domain, despite both domains being required for membrane targeting. Unexpectedly, ZnF, which possesses Ub-ligase activity and promotes Ras ubiquitination to attenuate the Ras signaling pathway (47), does not catalyze L1 ubiquitination, indicating that Rabex-5 Ub-ligase activity may exhibit substrate specificity. In the case of L1 endocytic trafficking, Rabex-5 functions as a UBP to ensure proper internalization and intracellular sorting, rather than as an E3 Ub-ligase.

In conclusion, this study into L1 down-regulation has provided novel information into the membrane trafficking mechanism by which the Rabex-5 UBP modulates expression of a neuronal cell adhesion molecule. The proposed Rabex-5-dependent endocytosis mechanism may be applicable to a broad spectrum of cell surface receptors, including the EGF receptor.

Acknowledgment—I thank Dr. V. Lemmon (University of Miami School of Medicine) for discussions on L1 biology.

REFERENCES

1. Maness, P. F., and Schachner, M. (2007) Neural recognition molecules of the immunoglobulin superfamily: signaling transducers of axon guidance and neuronal migration. *Nat. Neurosci.* **10,** 19–26
2. Schmid, R. S., and Maness, P. F. (2008) L1 and NCAM adhesion molecules as signaling coreceptors in neuronal migration and process outgrowth. *Curr. Opin. Neurobio1.* **18,** 245–250
3. Kamiguchi, H., Long, K. E., Pendergast, M., Schaefer, A. W., Rapoport, I., Kirchhausen, T., and Lemmon, V. (1998) The neural cell adhesion molecule L1 interacts with the AP-2 adaptor and is endocytosed via the clathrin-mediated pathway. *J. Neurosci.* **18,** 5311–5321
4. Kamiguchi, H., and Lemmon, V. (2000) Recycling of the cell adhesion molecule L1 in axonal growth cones. *J. Neurosci.* **20,** 3676–3686
5. Kamiguchi, H., and Yoshihara, F. (2001) The role of endocytic l1 trafficking in polarized adhesion and migration of nerve growth cones. *J. Neurosci.* **21,** 9194–9203
6. Wisco, D., Anderson, E. D., Chang, M. C., Norden, C., Boiko, T., Fölsch, H., and Winckler, B. (2003) Uncovering multiple axonal targeting pathways in hippocampal neurons. *J. Cell Biol.* **162,** 1317–1328
7. Yap, C. C., Nokes, R. L., Wisco, D., Anderson, E., Fölsch, H., and Winckler, B. (2008) Pathway selection to the axon depends on multiple targeting signals in NgCAM. *J. Cell Sci.* **121,** 1514–1525
8. Yap, C. C., Wisco, D., Kujala, P., Lasiecka, Z. M., Cannon, J. T., Chang, M. C., Hirling, H., Klumperman, J., and Winckler, B. (2008) The somatodendritic endosomal regulator NEEP21 facilitates axonal targeting of L1/NgCAM. *J. Cell Biol.* **180,** 827–842
9. Schaefer, A. W., Kamei, Y., Kamiguchi, H., Wong, E. V., Rapoport, I., Kirchhausen, T., Beach, C. M., Landreth, G., Lemmon, S. K., and Lemmon, V. (2002) L1 endocytosis is controlled by a phosphorylation-dephosphorylation cycle stimulated by outside-in signaling by L1. *J. Cell Biol.* **157,** 1223–1232
10. Dequidt, C., Danglot, L., Alberts, P., Galli, T., Choquet, D., and Thoumine, O. (2007) Fast turnover of L1 adhesions in neuronal growth cones involving both surface diffusion and exo/endocytosis of L1 molecules. *Mol. Biol. Cell* **18,** 3131–3143
11. Hicke, L., Schubert, H. L., and Hill, C. P. (2005) Ubiquitin-binding domains. *Nat. Rev. Mol. Cell Biol.* **6,** 610–621
12. Mukhopadhyay, D., and Riezman, H. (2007) Proteasome-independent functions of ubiquitin in endocytosis and signaling. *Science* **315,** 201–205
13. Raiborg, C., and Stenmark, H. (2009) The ESCRT machinery in endosomal sorting of ubiquitylated membrane proteins. *Nature* **458,** 445–452
14. Traub, L. M., and Lukacs, G. L. (2007) Decoding ubiquitin sorting signals for clathrin-dependent endocytosis by CLASPs. *J. Cell Sci.* **120,** 543–553
15. Dikic, I., Wakatsuki, S., and Walters, K. J. (2009) Ubiquitin-binding domains: from structures to functions. *Nat. Rev. Mol. Cell Biol.* **10,** 659–671
16. Haglund, K., and Dikic, I. (2012) The role of ubiquitylation in receptor endocytosis and endosomal sorting. *J. Cell Sci.* **125,** 265–275
17. Horiuchi, H., Lippé, R., McBride, H. M., Rubino, M., Woodman, P., Stenmark, H., Rybin, V., Wilm, M., Ashman, K., Mann, M., and Zerial, M. (1997) A novel Rab5 GDP/GTP exchange factor complexed to Rabaptin-5 links nucleotide exchange to effector recruitment and function. *Cell* **90,** 1149–1159
18. Mattera, R., Tsai, Y. C., Weissman A. M., and Bonifacino, J. S. (2006) The Rab5 guanine nucleotide exchange factor Rabex-5 binds ubiquitin (Ub) and functions as a Ub ligase through an atypical Ub-interacting motif and a zinc finger domain. *J. Biol. Chem.* **281,** 6874–6883
19. Lee, S., Tsai, Y. C., Mattera, R., Smith, W. J., Kostelansky, M. S., Weissman, A. M., Bonifacino, J. S., and Hurley, J. H. (2006) Structural basis for ubiquitin recognition and autoubiquitination by Rabex-5. *Nat. Struct. Mol. Biol.* **13,** 264–271
20. Delprato, A., Merithew, E., and Lambright, D. G. (2004) Structure, exchange determinants, and family-wide Rab specificity of the tandem helical bundle and Vps9 domains of Rabex-5. *Cell* **118,** 607–617
21. Lippé, R., Miaczynska, M., Rybin, V., Runge, A., and Zerial, M. (2001) Functional synergy between Rab5 effector Rabaptin-5 and exchange factor Rabex-5 when physically associated in a complex. *Mol. Biol. Cell* **12,** 2219–2228
22. Delprato, A., and Lambright, D. G. (2007) Structural basis for Rab GTPase activation by VPS9 domain exchange factors. *Nat. Struct. Mol. Biol.* **14,** 406–412
23. Haglund, K., Sigismund, S., Polo, S., Szymkiewicz, I., Di Fiore, P. P., and Dikic, I. (2003) Multiple monoubiquitination of RTKs is sufficient for their endocytosis and degradation. *Nat. Cell Biol.* **5,** 461–466
24. Long, K. E., Asou, H., Snider, M. D., and Lemmon, V. (2001) The role of endocytosis in regulating L1-mediated adhesion. *J. Biol. Chem.* **276,** 1285–1290
25. Diestel, S., Schaefer, D., Cremer, H., and Schmitz, B. (2007) NCAM is ubiquitylated, endocytosed, and recycled in neurons. *J. Cell Sci.* **120,** 4035–4049
26. Thelen, K., Georg, T., Bertuch, S., Zelina, P., and Pollerberg, G. E. (2008) Ubiquitination and endocytosis of cell adhesion molecule DM-GRASP regulate its cell surface presence and affect its role for axon navigation. *J. Biol. Chem.* **283,** 32792–32801
27. Schäfer, M. K., Schmitz, B., and Diestel, S. (2010) L1CAM ubiquitination facilitates its lysosomal degradation. *FEBS Lett.* **584,** 4475–4480
28. Damke, H., Baba, T., Warnock, D. E., and Schmid, S. L. (1994) Induction of mutant dynamin specifically blocks endocytic coated vesicle formation. *J. Cell Biol.* **127,** 915–934
29. Sakurai, T., Gil, O. D., Whittard, J. D., Gazdoiu, M., Joseph, T., Wu, J., Waksman, A., Benson, D. L., Salton, S. R., and Felsenfeld, D. P. (2008) Interactions between the L1 cell adhesion molecule and ezrin support

traction-force generation and can be regulated by tyrosine phosphorylation. *J. Neurosci. Res.* **86,** 2602–2614
30. Stenmark, H., Parton, R. G., Steele-Mortimer, O., Lütcke, A., Gruenberg, J., and Zerial, M. (1994) Inhibition of Rab5 GTPase activity stimulates membrane fusion in endocytosis. *EMBO J.* **13,** 1287–1296
31. Volpicelli, L. A., Lah, J. J., and Levey, A. I. (2001) Rab5-dependent trafficking of the m4 muscarinic acetylcholine receptor to the plasma membrane, early endosomes, and multivesicular bodies. *J. Biol. Chem.* **276,** 47590–47598
32. Dinneen, J. L., and Ceresa, B. P. (2004) Continual expression of Rab5(Q79L) causes a ligand-independent EGFR internalization and diminishes EGFR activity. *Traffic* **5,** 606–615
33. Mattera, R., and Bonifacino, J. S. (2008) Ubiquitin binding and conjugation regulate the recruitment of Rabex-5 to early endosomes. *EMBO J.* **27,** 2484–2494
34. Geetha, T., Jiang, J., and Wooten, M. W. (2005) Lysine 63 polyubiquitination of the nerve growth factor receptor TrkA directs internalization and signaling. *Mol. Cell* **20,** 301–312
35. Duncan, L. M., Piper, S., Dodd, R. B., Saville, M. K., Sanderson, C. M., Luzio, J. P., and Lehner, P. J. (2006) Lysine 63-linked ubiquitination is required for endolysosomal degradation of class I molecules. *EMBO J.* **25,** 1635–1645
36. Kumar, K. G., Barriere, H., Carbone, C. J., Liu, J., Swaminathan, G., Xu, P., Li, Y., Baker, D. P., Peng, J., Lukacs, G. L., and Fuchs, S. Y. (2007) Site-specific ubiquitination exposes a linear motif to promote interferon-α receptor endocytosis. *J. Cell Biol.* **179,** 935–950
37. Huang, F., Kirkpatrick, D., Jiang, X., Gygi, S., and Sorkin, A. (2006) Differential regulation of EGF receptor internalization and degradation by multiubiquitination within the kinase domain. *Mol. Cell* **21,** 737–748
38. Barriere, H., Nemes, C., Lechardeur, D., Khan-Mohammad M., Fruh, K., and Lukacs, G. L. (2006) Molecular basis of oligoubiquitin-dependent internalization of membrane proteins in mammalian cells. *Traffic* **7,** 282–297
39. Hawryluk, M. J., Keyel, P. A., Mishra, S. K., Watkins, S. C., Heuser, J. E., and Traub, L. M. (2006) Epsin 1 is a polyubiquitin-selective clathrin-associated sorting protein. *Traffic* **7,** 262–281
40. Traub, L. M. (2009) Tickets to ride: selecting cargo for clathrin-regulated internalization. *Nat. Rev. Mol. Cell Biol.* **10,** 583–596
41. Sorkina, T., Miranda, M., Dionne, K. R., Hoover, B. R., Zahniser, N. R., and Sorkin, A. (2006) RNA interference screen reveals an essential role of Nedd4–2 in dopamine transporter ubiquitination and endocytosis. *J. Neurosci.* **26,** 8195–8205
42. Jakobsson, J., Gad, H., Andersson, F., Löw, P., Shupliakov, O., and Brodin, L. (2008) Role of epsin 1 in synaptic vesicle endocytosis. *Proc. Natl. Acad. Sci. U.S.A.* **105,** 6445–6450
43. Sigismund, S., Woelk, T., Puri, C., Maspero, E., Tacchetti, C., Transidico, P., Di Fiore, P. P., and Polo, S. (2005) Clathrin-independent endocytosis of ubiquitinated cargos. *Proc. Natl. Acad. Sci. U.S.A.* **102,** 2760–2765
44. Donaldson, K. M., Yin, H., Gekakis, N., Supek, F., and Joazeiro, C. A. (2003) Ubiquitin signals protein trafficking via interaction with a novel ubiquitin binding domain in the membrane fusion regulator, Vps9p. *Curr. Biol.* **13,** 258–262
45. Carney, D. S., Davies, B. A., and Horazdovsky, B. F. (2006) Vps9 domain-containing proteins: activators of Rab5 GTPases from yeast to neurons. *Trends Cell Biol.* **16,** 27–35
46. Penengo, L., Mapelli, M., Murachelli, A. G., Confalonieri, S., Magri, L., Musacchio, A., Di Fiore, P. P., Polo, S., and Schneider, T. R. (2006) Crystal structure of the ubiquitin binding domains of Rabex-5 reveals two modes of interaction with ubiquitin. *Cell* **124**, 1183–1195
47. Yan, H., Jahanshahi, M., Horvath, E. A., Liu, H. Y., and Pfleger, C. M. (2010) Rabex-5 ubiquitin ligase activity restricts Ras signaling to establish pathway homeostasis in *Drosophila*. *Curr. Biol.* **20,** 1378–1382